

Dalton Transactions

Accepted Manuscript



This is an *Accepted Manuscript*, which has been through the Royal Society of Chemistry peer review process and has been accepted for publication.

Accepted Manuscripts are published online shortly after acceptance, before technical editing, formatting and proof reading. Using this free service, authors can make their results available to the community, in citable form, before we publish the edited article. We will replace this *Accepted Manuscript* with the edited and formatted *Advance Article* as soon as it is available.

You can find more information about *Accepted Manuscripts* in the [Information for Authors](#).

Please note that technical editing may introduce minor changes to the text and/or graphics, which may alter content. The journal's standard [Terms & Conditions](#) and the [Ethical guidelines](#) still apply. In no event shall the Royal Society of Chemistry be held responsible for any errors or omissions in this *Accepted Manuscript* or any consequences arising from the use of any information it contains.

COMMUNICATION

One-pot and one-step synthesis of bioactive Urease/ZnFe₂O₄ nanocomposites and their application in detection of urea

Cite this: DOI: 10.1039/x0xx00000x

Received 00th January 2014,
Accepted 00th January 2014

DOI: 10.1039/x0xx00000x

www.rsc.org/

Haitang Shi,^{ab} Xue Chen,^{ab} Linlin Li,^a Longfei Tan,^a Xiangling Ren,^a Jun Ren^a
and Xianwei Meng,^{*a}

This communication describes a novel environmentally-friendly method to prepare bioactive Urease/ZnFe₂O₄ nanocomposites through one-pot and one-step process. The synthetic procedure is triggered through a biological mineralization process of decomposition of urea catalyzed by urease. During the growth of ZnFe₂O₄, urease molecules are immobilized by original ZnFe₂O₄ nanoparticles. And as a consequence, the bioactive Urease/ZnFe₂O₄ nanoparticle composites are assembled. This simple route is expected to endow the bioactive nanocomposites with new properties for various interesting fields.

With the development of science and technology, biosensors are applied in more and more fields^[1], especially in clinical detection field. Immobilization of enzymes and proteins on activated supports permits the simplification of the biosensor design, which is a key technology for successful realization of enzyme-based biosensing processes.^[2] Innovative nanomaterials offer an exciting opportunity to address the challenges in immobilization of enzyme because of their large specific surface area and unique structure, which results in improved enzyme loading and enzyme activity compared to that of conventional materials. Recent breakthroughs in nano and hybrid technology have made various materials more affordable hosts for enzyme immobilization.^[3] Various enzymes have been immobilized on silica nanoparticles with multiple morphologies, including porous silica, mesoporous silica and Onion-like silica.^[4] Immobilization of the enzymes on gold nanoparticles is believed to help the protein to assume a favorable orientation and to make possible conducting channels between the prosthetic groups and the gold nanoparticle surface. Immobilized enzymes on magnetic nanoparticles exhibit high stability and can be easily separated from the reaction medium using a magnetic field.^[3]

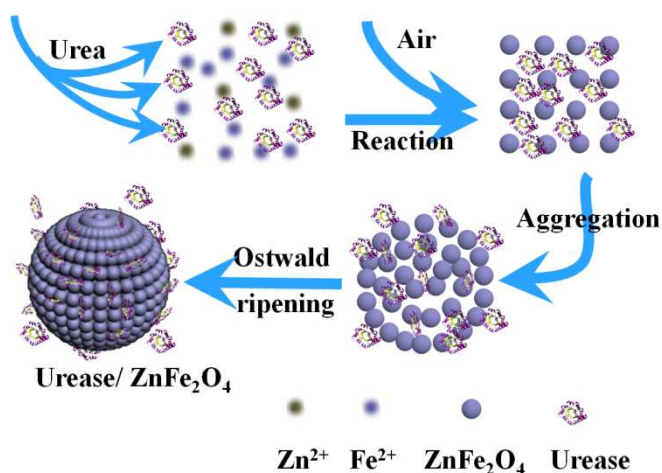
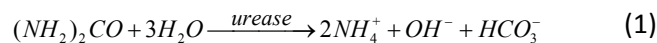
However, many state-of-the-art immobilization methods afford high-quality stabilized enzyme systems by post-immobilization of enzymes on pre-synthesized nanomaterials, namely, by a multi-step route, which is always very tedious and complex. The reasons

include that the preparation of nanomaterials is often conducted under rigorous conditions, e.g., high acidity, high temperature, and/or utilization of organic solvents, under which the enzymes may suffer severe deactivation.^[5] What's more, these methods often need some organic solvent or cross-linking agent,^[6] such as glutaraldehyde, during the immobilization process of enzyme. Thus, greater efforts are needed for manipulation of enzyme immobilization. Up to now, success on facile and efficient one-step preparation of nanomaterials-enzyme conjugates is very challenging and such success has not been achieved yet.

In this contribution, we develop a simple and environmentally-friendly method to prepare enzyme-zinc ferrite (Urease/ZnFe₂O₄) nanocomposites. The synthetic process is triggered through a biological mineralization process of decomposition of urea catalyzed by urease under mild conditions. During the growth of ZnFe₂O₄, urease molecules are immobilized by original ZnFe₂O₄ nanoparticles through electrostatic adsorption and covalent conjugation. And as a consequence, the bioactive Urease/ZnFe₂O₄ nanoparticle composites are assembled. The soft magnetic property of ZnFe₂O₄ endows the bioactive nanocomposites unique separable features for magnetic recycling. Our method overcomes the disadvantages of multi-step reaction and the use of organic solvent or cross-linking agent. The Urease/ZnFe₂O₄ nanocomposites can be used in biosensor to achieve sensitive detection of urea. This novel route is expected to endow the nanomaterials with new properties for various interesting applications.

During the synthetic process, the reactions (Equation 1~4) may happen to produce ZnFe₂O₄ nanoparticles.^[7] Urease is used to catalyse the decomposition of urea at mild temperature, which can keep the pH at a stable value due to the activity range of urease. Thus the reaction can act as a source of hydroxyls. When the pH is too high away from the optimal pH value, the catalytic activity of urease will be inhibited. The OH⁻

concentration will maintain at an appropriate range for the mineralization of crystalline ZnFe_2O_4 with uniform size.



Scheme 1. Schematic illustration of the growth mechanism of Urease/ ZnFe_2O_4 nanocomposites.

Scheme 1 illustrates the growth process of Urease/ ZnFe_2O_4 nanocomposites. Once the decomposition of urea starts to act as the source of hydroxyls (Equation 1), the precipitation reactions occur rapidly as Equation 2. Along with the continuous contact with air, ferrous hydroxides are oxidated and combined with zinc hydroxide to form original ZnFe_2O_4 nanoparticles with small size (Equation 3~4). During the process, urease just acts as a source of base, triggering the precipitation of ZnFe_2O_4 nanoparticles in the bulk solution. Once those newly born nanoparticles reach a critical size, they can self-assemble into transition spheres due to magnetic driven heterocoagulation process under mild conditions and short aging times. Meanwhile, urease also provides a useful interface for nucleation and growth of ZnFe_2O_4 nanoparticles with its high affinity to metal ions. During this process, some urease molecules can be encapsulated into the newly assembled transition spheres. As the reaction time continues, a typical ‘‘Ostwald ripening process’’ occurs, which results in ZnFe_2O_4 nanoparticles with larger size and higher crystallinity. The surface amination process of ZnFe_2O_4 nanoparticles may happen simultaneously due to the existence of ammonium ion. Subsequently, some excess urease molecules are combined onto the surface of ZnFe_2O_4 through electrostatic adsorption and covalent conjugation, and the final products of Urease/ ZnFe_2O_4 nanocomposites are obtained.

As shown in Figure 1a, the nanocomposites are almost spherical shape with nearly uniform diameter. Figure 1c represents the HRTEM image of Urease/ ZnFe_2O_4 nanocomposites, showing the spherical shape consistent well with the result of SEM images in

Figure 1a. Figure 1b represents the size distribution of Urease/ ZnFe_2O_4 nanocomposites, showing that the Urease/ ZnFe_2O_4 nanocomposites are very small to 23.88 ± 3.31 nm and the size distribution is rather narrow, which demonstrates the nearly uniform diameter well agreement with the visual results in Figure 1a. The lattice fringes can be seen very clearly in Figure 1c, in which the d-spacing of 0.253 nm, 0.484 nm is found to match well with the reflections from the (3 1 1), (1 1 1) peak of ZnFe_2O_4 , respectively. These results demonstrate that ZnFe_2O_4 nanoparticles have been successfully achieved with high crystallinity.

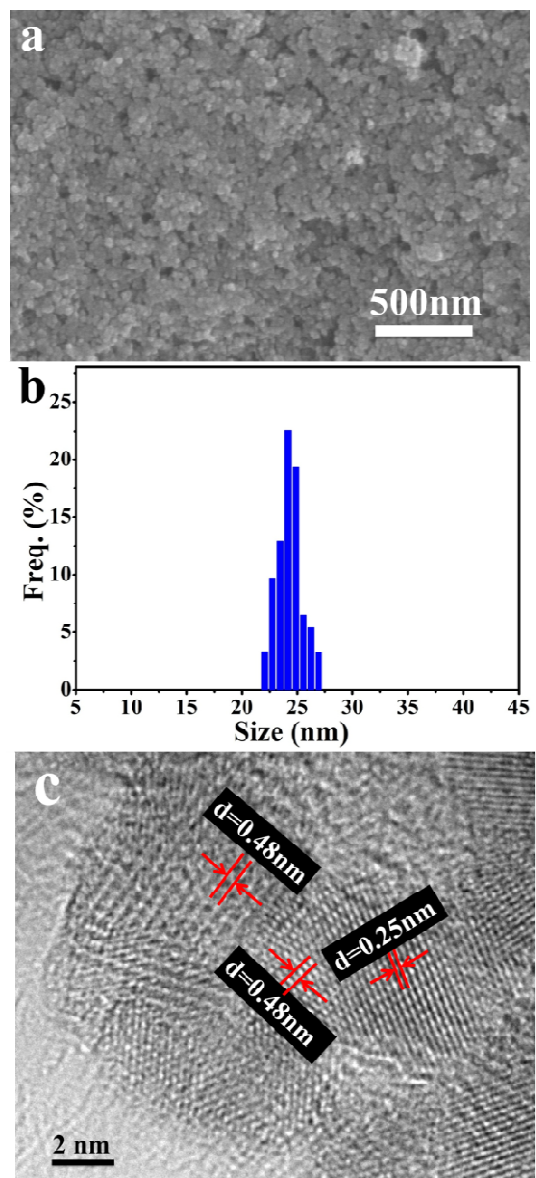


Figure 1. (a) SEM images, (b) size distribution, (c) HRTEM images of Urease/ ZnFe_2O_4 nanocomposites.

In Figure 2, the XRD data can prove the composition and phase purity of the as-prepared Urease/ ZnFe_2O_4 nanocomposites. The positions and relative intensities of the reflection peak are coincide well with the XRD patterns of ZnFe_2O_4 PDF card (22-1012). The characteristic peaks can be found at $2\theta=17.98^\circ$, 29.86° , 35.32° ,

42.95°, 56.44°, and 62.23° marked by their indices (1 1 1), (2 2 0), (3 1 1), (4 0 0), (5 1 1), and (4 4 0) respectively, which demonstrates that the as-prepared nanoparticles are indeed zinc ferrite crystal. The size (D), the inter-planar spacing (d_{hkl}), and the lattice parameter (a_{hkl}) of as-prepared nanoparticles can be calculated through the XRD spectra, which are shown in Table 1.^[7] The lattice parameters (a_{hkl}) of each lattice plane is almost similar and the value is approximately 0.84 nm, which can demonstrate the face-centred cubic structure of zinc ferrite crystal.

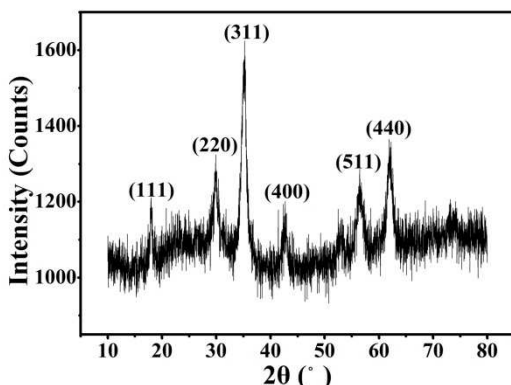


Figure 2. XRD pattern of Urease/ZnFe₂O₄ nanocomposites.

Table 1 The analysis results of XRD pattern.

(h k l)	(1 1 1)	(2 2 0)	(3 1 1)	(4 0 0)	(5 1 1)	(4 4 0)
$2\theta/^\circ$	17.98	29.86	35.32	42.95	56.44	62.23
B	1.151	1.092	1.152	1.072	1.329	1.257
D	6.910	7.445	7.157	7.875	6.708	7.300
d_{hkl}	0.484	0.299	0.253	0.210	0.163	0.149
a_{hkl}	0.8383	0.8457	0.8391	0.8400	0.8470	0.8429

Since different chemical state of Fe and Zn atoms in ZnFe₂O₄ can lead to different binding energies, and urease molecules pose massive Ni element, X-ray photoelectron spectra (XPS) was used to study the surface chemical compositions and the valence states of the nanocomposites as well as the successful combination of urease with ZnFe₂O₄. The full XPS spectrum of urease/ZnFe₂O₄ nanocomposites in Figure 3 confirms the existence of Zn, Fe, O and Ni elements. The binding energy peaks for Fe 2p and Fe 3p can be observed at ~710 eV and ~90 eV, respectively. Similarly the binding energy peaks for Zn 3d, Zn 3s, Zn 2p can be observed at ~10 eV, ~140 eV and ~1115 eV, respectively. The spectrum can also reflect the binding energy peaks of O 2s and O 1s at ~90 eV and ~600 eV, respectively. These results all indicate the formation of ZnFe₂O₄. The binding energy peaks for Ni 2p and Ni 2s can also be found in the full spectrum,

which may confirm the combination of urease with ZnFe₂O₄ nanoparticles.

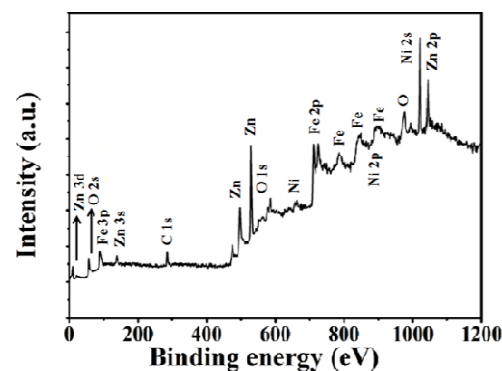


Figure 3. XPS pattern of Urease/ZnFe₂O₄ nanocomposites.

The magnetic hysteresis loops of the as-prepared Urease/ZnFe₂O₄ nanocomposites were measured and shown in Figure 4, compared with that of the pure ZnFe₂O₄ nanoparticles. The as-prepared Urease/ZnFe₂O₄ nanocomposites possess good soft magnetic properties with the saturation magnetization (M_s) of 7.58 emu g⁻¹, and near superparamagnetism properties with the remanent magnetization (M_R) of 0.1025 emu g⁻¹. These magnetic properties make the nanoparticles separable easily from mixture detection solution and recovery utilization with high-efficiency. While for the pure ZnFe₂O₄ nanoparticles, the saturation magnetization (M_s) can reach 8.31 emu g⁻¹, exceeding the M_s of Urease/ZnFe₂O₄ nanocomposites (7.58 emu g⁻¹). This may be contributed to the combination of urease and ZnFe₂O₄ and can be a proof of that urease has been well combined with ZnFe₂O₄ to obtain Urease/ZnFe₂O₄ nanocomposites.

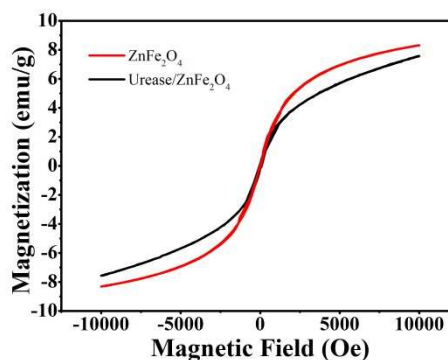


Figure 4. Magnetic curves of ZnFe₂O₄ and Urease/ZnFe₂O₄ nanocomposites.

These characterizations, including the proof of UV-Vis spectra in Figure S1, all confirm the successful fabrication of Urease/ZnFe₂O₄ nanocomposites with various desirable properties, including the property of soft magnetic and catalytic hydrolysis of urea under ambient conditions.

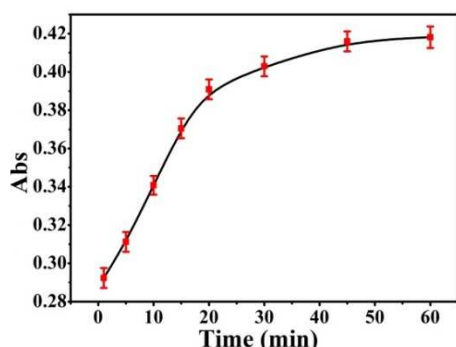


Figure 5. Time-dependent absorbance changes at 588 nm of bromocresol purple (8 mg L^{-1}) in the presence of equivalent Urease/ZnFe₂O₄ nanocomposites (5 mg ml^{-1}) and urea (50 mM).

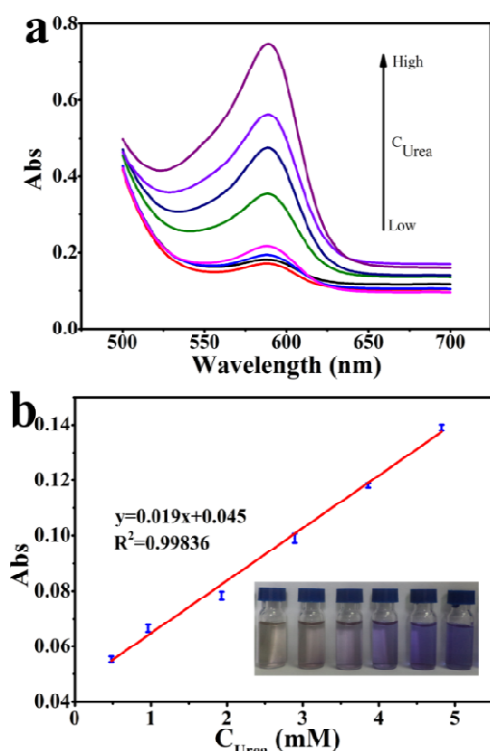


Figure 6. (a) UV-Vis spectra of the supernatant solution containing bromocresol purple after addition of the mixture of urea ($0.01 \sim 5 \text{ mM}$) and equivalent Urease/ZnFe₂O₄ nanocomposites (5 mg ml^{-1}), (b) the response curve of the urea concentrations in the presence of equivalent Urease/ZnFe₂O₄ nanocomposites (5 mg ml^{-1}). Inset: Images of production of colored products for different concentrations of urea ($0.01 \sim 5 \text{ mM}$).

Figure 5 represents the time influence to the detection procedure, showing that during the first 30 minutes, the catalytic reaction keeps proceeding rather fast. With the extension of reaction time, the catalytic reaction slows down gradually due to the saturation of urease or the exhaustion of urea probably. On account of the time influence, each detection procedure in this work was kept in 30 minutes to achieve the best effect.

Figure 6a displays the UV-Vis spectra of the supernatant containing bromocresol purple after addition of the mixture of urea

and Urease/ZnFe₂O₄ nanocomposites. The value of peak increases with the increase of the concentration of urea. Figure 6b reveals the calibration curve of the concentration of urea. A good linearity can be obtained in the range of $0.01 \sim 5 \text{ mM}$, with a detection limit of $10 \mu\text{M}$ urea, and the regression equation can be calculated through $y = 0.019x + 0.045$ with a high correlation coefficient of 0.99836. The value of detection limit is as low as reported in some previous literatures^[1b,8] and even much lower than that of some previous literatures^[9], and the detection range is wide enough from the level of μM to mM . The inset of Figure 6b is the visual detection of urea using the Urease/ZnFe₂O₄ nanocomposites, showing that with the rise of the concentration of urea solution, the colour of the mixture changes from light yellow to purple and the purple becomes deeper and deeper.

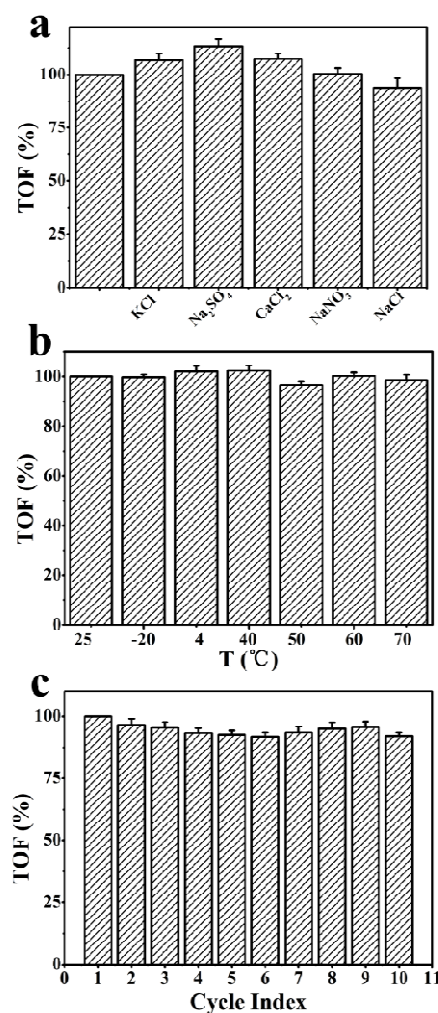


Figure 7. (a) Anti-interference results by different ions, including K^+ , Na^+ , Ca^{2+} , Cl^- , which may be mainly exist in real samples (b) temperature stability of Urease/ZnFe₂O₄ nanocomposites after being placed at -20 , 4 , 25 , 40 , 50 , 60 , and $70 \text{ }^\circ\text{C}$ for 1 h respectively, and (c) repeating utilization rate of Urease/ZnFe₂O₄ nanocomposites after the detection procedure being repeated for 10 times. Samples were the mixture of 8 mg L^{-1} bromocresol purple, 50 mM urea and 5 mg ml^{-1} Urease/ZnFe₂O₄ nanocomposites.

The feasibility of the detection based on the as-prepared Urease/ZnFe₂O₄ nanocomposites was evaluated by monitoring the anti-interference performance with the existence of other ions, including KCl, Na₂SO₄, CaCl₂, NaNO₃ and NaCl, which may be mainly exist in real samples (Figure 7a). Comparing with the control group, the interference caused by these ions could be negligible, indicating that the Urease/ZnFe₂O₄ nanocomposites can be used in many complex environments to achieve the detection of urea.

In order to explore the temperature stability of the as-prepared Urease/ZnFe₂O₄ nanocomposites, the nanocomposites were placed at -20, 4, 25, 40, 50, 60, and 70 °C for 1 h respectively. Subsequently the detection procedure was repeated at same conditions. As shown in Figure 7b, the catalytic property almost keeps constant regardless of temperature, indicating that the as-prepared Urease/ZnFe₂O₄ was rather stable. The good temperature stability also makes the as-prepared Urease/ZnFe₂O₄ nanocomposites be well applied in more harsh conditions.

The Urease/ZnFe₂O₄ nanocomposites were tested for its reproducibility by a typical cyclic process as follow: after each detection process, the Urease/ZnFe₂O₄ nanocomposites were separated from the solution by a magnet and washed with deionized water for 3~5 times. Subsequently the detection procedure was repeated again for 10 times. Figure 7c expounds the cyclic utilization rate of the as-prepared nanocomposites and compares the efficiency each time with the first time, showing that the efficiency can still reach 91.91% when the cycle index reaches 10 times. During each cycle, urea solutions have less effect on catalytic property of urease and the role of ZnFe₂O₄ is only to make the bioactive nanocomposites be separated easily from the base solutions. Figure 7c shows the high cyclic utilization rate of the as-prepared Urease/ZnFe₂O₄ nanocomposites.

Some other advantages of Urease/ZnFe₂O₄ nanocomposites in the detection of urea are discussed in Figure S2 and Figure S3, including the tolerance to pH and air-dry.

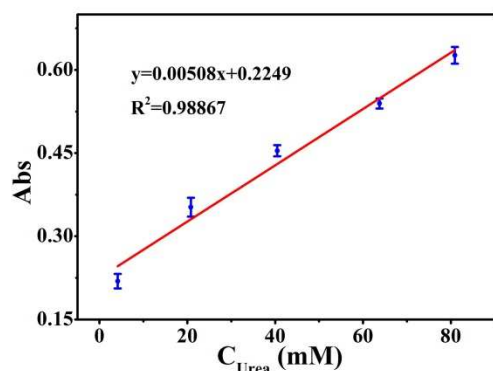


Figure 8. The calibration curve detected in milk.

To better analyze the possibility application of the as-prepared Urease/ZnFe₂O₄ nanocomposites in physical condition, we choose milk as practical detective sample to achieve the same detection. The calibration curve of urea in milk is as shown in Figure 8, with the linear response of 4~80 mM and high correlation coefficient of

0.98867. The linear regression equation is $y=0.00508x+0.2249$, where x is the concentration of urea solutions and y the ultraviolet absorption values. There were no significant interferences with other substances in milk samples. These works further prove that the as-prepared Urease/ZnFe₂O₄ nanocomposites own huge potential application in the detection of urea, especially in the reality that urea is a toxic pollutant causing serious biological disorders when added into some dairy products (e.g. milk).^[9d]

In conclusion, bioactive Urease/ZnFe₂O₄ nanocomposites were prepared through a one-pot, one-step and environmentally-friendly method, during which there had not any other organic solvent or cross-linking agent added into the reaction mixture. Compared with the existing methods of preparing bioactive nanocomposites, our method can shorten the synthetic steps from multi-steps to one-step, making the synthetic process simple and convenient. Due to the soft magnetic properties and bioactive catalytic properties, the as-prepared Urease/ZnFe₂O₄ nanocomposites can be well applied to the detection of urea with high detection efficiency, recovery utilization efficiency and anti-interference performance.

Experimental section

Preparation of Urease/ZnFe₂O₄ nanocomposites

The detail process of preparing Urease/ZnFe₂O₄ nanocomposites is as follows, Zinc chloride (ZnCl₂) and Ferrous chloride (FeCl₂·4H₂O) were dissolved in deionized water in a 3-neck flask, which was heated to 60 °C with lasting mechanical stirring and urease solution (1 mg/mL) was added. Then, urea was added into the solution to trigger the catalytic and synthetic reaction. The reaction temperature was kept at 60 °C for an hour. The products were separated with a magnet and washed for 3 times with deionized water. The final products were preserved at 4 °C to maintain the biological catalytic activity.

The detection procedure of urea

During the detection procedure of urea, a kind of pH-sensitive dye, bromocresol purple,^[10] was used to monitor the change of pH value of the sample to achieve the detection of urea. The absorbance at 588 nm can increase linearly with pH value within the range of 5.8 to 7.5.^[10a] The experimental process is as below: Urease/ZnFe₂O₄ nanocomposites solution was added into urea solutions with different concentration. Subsequently, the mixture solution was incubated in a water bath of 30 °C for 30 minutes. Urease/ZnFe₂O₄ nanocomposites were separated from the mixture solution by a magnet and bromocresol purple solution was added into the supernatant fluid. UV-Vis adsorption spectra of the mixture solution were measured subsequently.

Acknowledgements

This work was supported by the National Natural Science Foundation of China (Project No. 81171454, 61171049, and 60907042) and we sincerely express our thanks here.

Notes and references

^a Laboratory of Controllable Preparation and Application of Nanomaterials, Research Center for Micro&Nano Materials and Technology, Technical Institute of Physics and Chemistry, Chinese Academy of Sciences, Beijing 100190, People's Republic of China.

^b University of Chinese Academy of Sciences, Beijing 100049, People's Republic of China.

† Footnotes should appear here. These might include comments relevant to but not central to the matter under discussion, limited experimental and spectral data, and crystallographic data.

Electronic Supplementary Information (ESI) available: [details of any supplementary information available should be included here]. See DOI: 10.1039/c000000x/

T. M. Pan, *Anal. Chim. Acta*, 2009, **651**, 36; d) G. P. Nikoleli, D. P. Nikolelis and C. Methenitis, *Anal. Chim. Acta*, 2010, **675**, 58.
[10] a) Y. Lvov, A. A. Antipov, A. Mamedov, H. Möhwald and G. B. Sukhorukov, *Nano Lett.*, 2001, **1**, 125; b) W. Yao and R. H. Byrne, *Environ. Sci. Technol.*, 2001, **35**, 1197; c) Y. Lvov and F. Caruso, *Anal. Chem.*, 2001, **73**, 4212.

- [1] a) Y. C. Luo and J. S. Do, *Biosens. Bioelectron.*, 2004, **20**, 15; b) C. P. Huang, Y. K. Li and T. M. Chen, *Biosens. Bioelectron.*, 2007, **22**, 1835; c) S. K. Jha, M. Kanungo, A. Nath and S. F. D. Souza, *Biosens. Bioelectron.*, 2009, **24**, 2637.
- [2] a) C. Mateo, V. Grazu, J. M. Palomo, F. L. Gallego, R. F. Lafuente and J. M. Guisan, *Nat. Protoc.*, 2007, **2**, 1022; b) L. Cao, L. Langen and R. A. Sheldon, *Curr. Opin. Biotech.*, 2003, **14**, 387; c) A. I. Kallenberg, F. Rantwijk and R. A. Sheldon, *Adv. Synth. Catal.*, 2005, **347**, 905; d) L. Cao, F. Rantwijk and R. A. Sheldon, *Org. Lett.*, 2000, **2**, 1361.
- [3] E. T. Hwang and M. B. Gu, *Eng. Life Sci.*, 2013, **13**, 49.
- [4] a) A. Popat, S. B. Hartono, F. Stahr, J. Liu, S. Z. Qiao and G. Qing, *Nanoscale*, 2011, **3**, 2801; b) J. Sun, H. Zhang, R. Tian, D. Ma, X. Bao, D. S. Su and H. Zou, *Chem. Commun.*, 2006, 1322.
- [5] Y. Fu, P. Li, Q. Xie, X. Xu, L. Lei, C. Chen, C. Zou, W. Deng and S. Yao, *Adv. Funct. Mater.*, 2009, **19**, 1784.
- [6] a) N. Vasylieva, C. Maucler, A. Meiller, H. Viscogliosi, T. Lieutaud, D. Barbier and S. Marinesco, *Anal. Chem.*, 2013, **85**, 2507; b) T. Honda, M. Miyazaki, H. Nakamura and H. Maeda, *Chem. Commun.*, 2005, 5062; c) K. Gabrovska, J. Ivanov, I. Vasileva, N. Dimova and T. Godjevargova, *Int. J. Biol. Macromol.*, 2011, **48**, 620; d) X. Chen, Z. Yang and S. Si, *J. Electroanal. Chem.*, 2009, **635**, 1; e) İ. Bozgeyik, M. Şenel, E. Çevik and M. F. Abasiyanik, *Curr. Appl. Phys.*, 2011, **11**, 1083; f) S. K. Kirdeciler, E. Soy, S. Ozturk, I. Kucherenko, O. Soldatkin, S. Dzyadevych and B. Akata, *Talanta*, 2011, **85**, 1435; g) X. Wang, Z. Jiang, J. Shi, Y. Liang, C. Zhang and H. Wu, *ACS Appl. Mater. Inter.*, 2012, **4**, 3476; h) J. Kobayashi, Y. Mori and S. Kobayashi, *Chem. Commun.*, 2006, 4227.
- [7] a) H. S. Qian, Y. Hu, Z. Q. Li, X. Y. Yang, L. C. Li, X. T. Zhang and R. Xu, *J. Phys. Chem. C*, 2010, **114**, 17455; b) Z. Liu, T. Fan, H. Zhou, D. Zhang, X. Gong, Q. Guo and H. Ogawa, *Bioinspir. Biomim.*, 2007, **2**, 30; c) Y. Cao, D. Jia, P. Hu and R. Wang, *Ceram. Int.*, 2013, **39**, 2989; d) Y. Ding, Y. Yang and H. Shao, *Electrochim. Acta*, 2011, **56**, 9433; e) M. Jean and V. Nachbaur, *J. Alloy. Compd.*, 2008, **454**, 432; f) O. M. Lemine, M. Bououdina, M. Sajjedine, A. M. Alsaie, M. Shafi, A. Khatab, M. Alhilali and M. Henini, *Physica B*, 2011, **406**, 1989.
- [8] R. Sahney, S. Anand, B. K. Puri and A. K. Srivastava, *Anal. Chim. Acta*, 2006, **578**, 156.
- [9] a) S. Srivastava, P. R. Solanki, A. Kaushik, M. A. Ali, A. Srivastava and B. D. Malhotra, *Nanoscale*, 2011, **3**, 2971; b) H. D. Duong and J. I. Rhee, *Anal. Chim. Acta*, 2008, **626**, 53; c) M. H. Wu, C. D. Lee and

One-pot and one-step synthesis of bioactive Urease/ ZnFe_2O_4 nanocomposites and their application in detection of urea

Haitang Shi, Xue Chen, Linlin Li, Longfei Tan, Xiangling Ren, Jun Ren, and Xianwei Meng

This paper describes a simple method to prepare bioactive Urease/ ZnFe_2O_4 nanocomposites, and explores their application in sensitive detection of urea.

